ADVANCED QUANTUM TECHNOLOGIES
www.advquantumtech.com

Quantum Entanglement Among Multiple Memories for Continuous Variables

Zhihui Yan, Liang Wu, Xiaojun Jia, Changde Xie, and Kunchi Peng*

Quantum network is constituted by quantum channels and quantum nodes. The interaction between non-classical optical modes and quantum nodes, as well as quantum entanglement among multiple distant quantum nodes are the building blocks of quantum network, which enable to achieve a plethora of quantum information protocols, such as distributed quantum computation, quantum state transfer across quantum nodes, and quantum clock network. On one hand, the multipartite non-classical states of optical modes, which can directly interact with atomic ensembles, are required for the practical applications of quantum network. On the other hand, a crucial goal of quantum network is to unconditionally generate and on-demand store and retrieve multipartite entangled states in atomic ensembles. This paper presents an up-to-date review on recent developments in these areas: multipartite continuous-variable polarization entangled optical modes have been created by transforming quantum state from quadrature into polarization components; and a scalable quantum network with deterministic entanglement among multiple quantum memories has been constructed by transferring spatially separated entangled optical modes into atomic ensembles.

1. Introduction

Quantum network consisting of quantum channels and quantum nodes attracts more and more attentions due to its advantages of outperforming the classical approaches. Light is an ideal carrier of quantum information because of fast transmission speed and weak interaction with the environment. Quantum channels, such as optical fibers and orbiting satellites, can transmit quantum information carried by quantum state of light across quantum network and interconnect the quantum nodes to construct a large scale quantum network.[1,2] Meanwhile, a multitude of physical systems can be used as quantum nodes to store and process quantum information, such as atomic ensembles,[3–7] single atoms,[8,9] trapped ions,[10,11] opto-mechanics,[12–15] superconductors,[16] and crystals.[17,18] Atomic ensembles with large optical depth and good quantum coherence are one of the candidates of quantum nodes. The non-classical states, such as squeezing and entanglement, are not only the kernel concepts of quantum mechanics, but also the essential resources of quantum information technology,[19–21] such as quantum teleportation,[22,23] quantum entanglement swapping,[24–26] quantum secret sharing,[27–29] quantum computation,[30,31] and quantum metrology.[32] Squeezed state can significantly reduce quantum noise to be below quantum noise limit (QNL),[33] and for entanglement state there exist non-local quantum correlations between two sub-systems or among more sub-systems.[34] According to the observables with the discrete and continuous eigenvalues, quantum information is divided into discrete variable (DV) and continuous variable (CV) approaches. The DV quantum information takes the advantages of high fidelity, while in the CV regime it can implement the deterministic quantum information applications, both of which have been rapidly developed in parallel.

The interaction between non-classical optical mode and quantum node is demanding for storing the flying quantum states of light in stationary quantum nodes. Both the spin of atoms and polarization of optical modes are described by Stokes operators of Bloch and Poincare spheres, respectively. Thus the collective spins of atoms and polarizations of optical modes can directly interact with each other, and quantum variance can be directly transferred between the polarizations of optical modes and spins of atomic spin waves. While the quantum DV polarization states have been widely employed in quantum information technology,[19] the CV polarization entangled states with efficient generation, manipulation and local oscillator free measurement provide another avenue for implementing quantum network.[35] The non-classical CV polarization state of light has advantages in the applications of quantum communications and quantum memory.[36,37] In a large scale quantum network, the phase fluctuation of locking interference signal is large when the signal and local oscillation modes go through the long-distance fiber

Z. Yan, L. Wu, X. Jia, C. Xie, K. Peng
State Key Laboratory of Quantum Optics and Quantum Optics Devices
Institute of Opto-Electronics
Shanxi University
Taiyuan 030006, P. R. China
E-mail: jiaxj@sxu.edu.cn
Z. Yan, L. Wu, X. Jia, C. Xie, K. Peng
Collaborative Innovation Center of Extreme Optics
Shanxi University
Taiyuan 030006, P. R. China

The ORCID identification number(s) for the author(s) of this article can be found under https://doi.org/10.1002/qute.202100071

DOI: 10.1002/qute.202100071

or long lifetime memory medium, respectively. The local oscillator free measurement of CV polarization components can overcome this problem. Besides, the spin squeezing of atomic ensembles can be generated by transferring squeezed state from optical mode into atomic ensemble, which can be used in quantum metrology. Therefore, a variety of efforts have been done to produce non-classical CV polarization states of optical modes. In 2002, the concept of the CV polarization squeezing has been proposed,[38] which can interact with atomic spin wave directly and be measured conveniently.[39] The CV polarization squeezing matching optical fiber transmission window has been generated by means of an asymmetric fiber-optic Sagnac interferometer,[40] and the CV polarization squeezed state resonant with cesium atomic absorption line has been produced by using a cloud of cold cesium atoms in a high-finesse optical cavity.[41] Together with the optical beam splitter network, the well understood optical parametric amplifiers (OPAs) have been used to generate CV polarization squeezed state resonant with rubidium atomic absorption line, whose quantum noises of three Stokes operators are all −4.0 dB below QNL.[42] The bipartite CV polarization entanglement has been theoretically proposed and experimentally investigated.[35,43–45] With the development of quantum network, the multipartite CV polarization entanglement is required for the multiple users in quantum network, which can transfer quantum state between quantum nodes in quantum network, and the direct interaction between atomic spin waves and polarization components of optical modes. The CV tripartite polarization entangled state of optical modes resonant on the rubidium absorption line has been obtained by transforming the tripartite quadrature GHZ-like entangled state into polarization entangled state. According to the inseparability criterion and the genuine criterion extended for the multipartite CV polarization entanglement,[46,47] both criteria are violated, which demonstrate the tripartite CV polarization entangled state is generated. This system can also be directly extended to generate CV polarization entangled states with more optical modes.[48]

Quantum memory, which can write and store quantum state of flying optical mode in stationary matter system and on demand read quantum state from matter to released optical mode, is the building block of practical applications of quantum network protocols. In a large scale quantum internet, the loss and decoherence are unavoidable which limit the distance of quantum communication. Quantum repeater can divide long distance entanglement distribution into short distance segments consisting of entanglement preparation, purification, memory and interconnect to solve the problem of the loss and decoherence in a large scale quantum internet.[49] In quantum memory, the memory efficiency and noise influence the successful building of a quantum repeater. The implementation of entangled nodes with high generation rate and high entangled degree requires high memory efficiency. Also the correlation variance is very sensitive to the memory noise, which will destroy the quantum entanglement. In quantum repeater, long storage time can extend the distance of each segment. If the performance of quantum memory is better, the fewer segments resources of quantum repeater are required for practical longer distance and higher entangled quantum repeater. Besides, atomic ensemble based quantum memory enables to implement distributed quantum computation and quantum enhanced atomic magnetometry.[50,51] The controlled-phase gates can be implemented by using four quantum memory nodes with a cluster-state, and is the essential integral of one way quantum computation.[50] Spin squeezing holds the promise to realize sub-QNL sensitivity of atomic magnetometry.[51] Therefore, there are varieties of progresses on quantum memories, which employ different kinds of light and atom interaction mechanisms, such as electromagnetically induced transparency (EIT),[52–54] quantum non-demolition (QND),[55] gradient echo memory,[56,57] DLCZ protocols,[58,59] controlled reversible inhomogeneous boarding (CRIB), and atomic frequency comb (AFC).[60] The EIT memory with low excess memory noise is a well understood memory device, which is suitable for non-classical state of optical mode, as well as quantum memories for squeezed and entangled states have been demonstrated based on EIT interaction.[36,61,62]

To establish and store quantum entanglement in quantum nodes and then to controllably release the stored entangled state from quantum nodes to released optical modes in quantum channels are required for quantum computation and quantum communication.[63–65] By using Raman scattering[66] or quantum states transferring from entangled photons into atomic ensembles,[67–69] the entanglements between two atomic ensembles have been experimentally completed. How to entangle more quantum nodes across quantum network is the core problem of the quantum network. In Raman scattering scheme, the multiple pairs of hybrid entanglements between atom and photon are interfered and measured to induce the heralded entanglement among multiple atomic ensembles. The measurement-induced entanglement among four atomic ensembles have been demonstrated, which proved that a quadripartite W state of atomic ensembles can be obtained.[70] By transferring the W state of atomic spin waves into a photonic modes the multipartite entanglement can be verified or distributed across quantum networks. The entanglement of three remote quantum memories via three-photon interference have been experimentally realized.[71] The atomic ensemble and photon entanglement is realized by using a ring cavity to enhance the overall efficiency. By interfering three single photons entangled with three atomic ensembles, measuring the photons and applying feed forward, the heralded entanglement between the three atomic ensembles has been achieved. To entangle more quantum nodes is the core problem of the quantum network. The successful rate of entanglement generation mainly limits the number of entangled nodes. And the CV quantum information with the deterministic advantage can effectively entangle more quantum nodes by storing more entangled optical modes. Besides DV entanglement schemes of atomic ensembles, the CV regime provides another method of the realization of quantum information protocols. The CV entanglement between two atomic ensembles has been experimentally realized by using QND measurement[72] and dissipation mechanism,[73] respectively. Alternatively, two atomic ensembles can be entangled by storing two sideband modes of entangled state.[36] In CV regime, the entangled two sideband modes are used to create entanglement between two atomic ensembles based on QND interaction. The number of entangled sideband modes with different frequency shifts is restricted by the bandwidth of optical parametric amplifier. And it is also difficult to spatially separate these entangled optical sideband modes with small frequency intervals. These limitations make it difficult

to entangle more atomic ensembles. Quantum variance can be transferred between the spatially septated CV entangled optical modes and atomic ensembles, which can deterministically generated large scale quantum entanglement among quantum nodes. In 2017, three atomic ensembles have been deterministically entangled in a GHZ-like state by transferring CV entangled state from spatially septated optical modes to distant atomic ensembles based on EIT mechanism.[74] First, a tripartite GHZ-like entangled state is off-line prepared by means of three OPAs and optical beam splitter network. Based on the EIT interaction, these three entangled optical modes are stored in three atomic ensembles located 2.6 m apart from each other. After a given storage time, the entanglement is controllably released from atomic ensembles into three spatially separated optical modes. Quantum state transferring approach from spatially separated optical modes to atomic ensembles enables to entangle more atomic ensembles. The better quality of multiple entangled quantum nodes can be obtained if higher entangled optical modes and better performance quantum memory are employed. And thus the CV quantum system is suitable for constructing multiple-user quantum network.

This review discusses the recent developments in quantum network involving the non-classical optical modes and atomic ensembles. We focus on generation of non-classical CV polarization states of optical modes, including CV polarization squeezing and multipartite CV polarization entanglement. In addition, we review the state-of-the-art experimental developments quantum storage and retrieval of non-classical optical mode and entanglement generation in atomic ensembles. Particularly, we study the quantum state transfer approaches for entangling multiple atomic ensembles.

2. Production of CV Polarization Non-Classical States of Optical Modes

Spin components of atoms are expressed in the Bloch sphere, while polarization components of light is represented in Poincare sphere. Both spin of atoms and polarization of optical mode are described by Stokes operators, and they can interact with each other directly. The measurements of the Stokes operators are independent of local oscillator of balanced homodyne detection (BHD).

In quantum optics, the polarization components are represented by Stokes operators ($\hat{S}_0$, $\hat{S}_1$, $\hat{S}_2$ and $\hat{S}_3$), which constitute a Poincare sphere.[38] Stokes operator $\hat{S}_0$ means the intensity, and $\hat{S}_1$, $\hat{S}_2$ and $\hat{S}_3$ represent the three polarizations which form a Cartesian axes system. The Stokes parameters for pure states can be expressed by the annihilation $\hat{a}_{\mathrm{H(V)}}$ and creation $\hat{a}^{+}_{\mathrm{H(V)}}$ operators of the horizontally (subscript H) and vertically (subscript V) polarized modes, as

$$\hat{S}_0 = \hat{a}^{+}_{\mathrm{H}}\hat{a}_{\mathrm{H}} + \hat{a}^{+}_{\mathrm{V}}\hat{a}_{\mathrm{V}}, \tag{1}$$

$$\hat{S}_1 = \hat{a}^{+}_{\mathrm{H}}\hat{a}_{\mathrm{H}} - \hat{a}^{+}_{\mathrm{V}}\hat{a}_{\mathrm{V}},$$

$$\hat{S}_2 = \hat{a}^{+}_{\mathrm{H}}\hat{a}_{\mathrm{V}}e^{i\theta} + \hat{a}^{+}_{\mathrm{V}}\hat{a}_{\mathrm{H}}e^{-i\theta},$$

$$\hat{S}_3 = (\hat{a}^{+}_{\mathrm{H}}\hat{a}_{\mathrm{V}}e^{i\theta} - \hat{a}^{+}_{\mathrm{V}}\hat{a}_{\mathrm{H}}e^{-i\theta})/i$$

where θ is the relative phase between the horizontal and vertical polarization modes.

2.1. Generation of CV Polarization Squeezed State of Optical Mode

Squeezed state is the key resource in applications of quantum information, which can realize the precision measurement with the sensitivity beyond the classical approach.[75,76] Laser interferometer is a powerful precision measurement tool for gravitational wave observation, and squeezed state has been injected into the unused port of laser interferometer to improve the sensitivity.[77,78] The CV polarization squeezed states of light, which is demanding for quantum network, have been theoretically and experimentally investigated. For long distance quantum communication, the polarization squeezed state matching the transmission window of optical fiber has been obtained by using asymmetric fiber Sagnac interferometer, and has been distributed through the atmosphere channels.[37] With the development of the interaction between non-classical light and matter, the non-classical states of optical modes resonant with the atomic absorption are required, which are the base of quantum information processing and memory. The polarization squeezing state of light resonant with cesium atomic absorption line has been generated in high finesse optical cavity.[41] Besides, OPA is a well-understood quantum device to generate non-classical state of optical mode. By coupling two quadrature squeezed modes generated from the sub-threshold OPAs with the strong coherent states on a polarization beam splitter, the CV polarization squeezing can be obtained.[39] The CV polarization squeezing resonant with D1 absorption line of rubidium can directly interact with rubidium atoms and be measured only by half wave plate, quarter wave plate and polarization beam splitter (PBS). Thus the polarization squeezed state of light resonant with rubidium atom D1 absorption has been generated based on sub-threshold OPAs and beam splitting network.[42] The operator can be considered as the sum of the mean value and the variance. Two quadrature amplitude squeezed optical modes with the same power and orthogonal polarization are coupled on a PBS with zero phase difference. The variances of each Stokes operator are expressed as

$$V_0 = V_1 = \alpha^2(\Delta^2\hat{X}_{\mathrm{H}} + \Delta^2\hat{X}_{\mathrm{V}}), \tag{2}$$

$$V_2(\theta) = \cos^2\theta\alpha^2(\Delta^2\hat{X}_{\mathrm{H}} + \Delta^2\hat{X}_{\mathrm{V}}) + \sin^2\theta\alpha^2(\Delta^2\hat{Y}_{\mathrm{H}} + \Delta^2\hat{Y}_{\mathrm{V}}),$$

$$V_3(\theta) = V_2(\pi/2 - \theta)$$

where $\hat{X}_{\mathrm{H(V)}}$ and $\hat{Y}_{\mathrm{H(V)}}$ are quadrature amplitude and phase of horizontal (vertical) polarization modes, respectively. Therefore, the three Stokes operators can be simultaneously squeezed by coupling two quadrature amplitude squeezed state V_0, V_1, and V_2 will be less than QNL.

Figure 1 shows the schematic of generating polarization squeezed optical mode.[42] A Ti:Sapphire laser outputs 795 nm laser, which is used to be the fundamental wave of external cavity enhanced second harmonic genetation (SHG), input signal optical modes of two OPAs and two strong coherent states of optical modes. The 398 nm laser generated by external cavity enhanced SHG is used to pump two identical OPAs for generating two

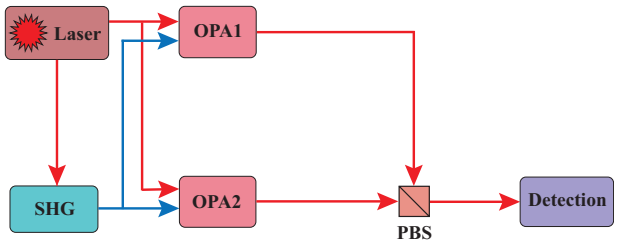

Figure 1. Schematic of generating polarization squeezed optical mode. Laser system, a titanium sapphire laser pumped by green laser; SHG system, an external cavity enhanced second harmonic generator; OPAs, optical parametric amplifiers; PBS, polarization beam splitters; detection system, measurement of Stokes operators of optical modes.

beams of 795 nm quadrature squeezed state of optical modes. The 398 nm laser is generated by external cavity enhanced SHG with a four-mirror ring cavity configuration, consisting of two flat mirrors, two spherical mirrors with 100 mm radius of curvature, and a $1 \times 2 \times 10$ mm^3 type-0 phase-matching PPKTP crystal. The flat mirror with transmissivity of 13.0% at 795 nm is used as the input coupler of the SHG. The SHG cavity is locked to be resonance with the input fundamental wave by the Pound–Drever–Hall (PDH) technique. The maximum output power of cavity enhanced SHG is 380 mW laser at 398 nm, when the input fundamental wave power is 1 W. While the fundamental wave power is reduced to 627 mW, the cavity enhanced SHG stably outputs 279 mW laser at 398 nm. Both the two OPAs with the same four-mirror ring cavity configuration as that of SHG cavity. The spherical mirrors with antireflection at 398 nm and high-reflection at 795 nm are used as the input couplers of the OPAs. The flat mirrors with transmissivity of 5.0% for 795 nm are used as the output couplers. The resulting two quadrature squeezed optical fields are transformed into polarization squeezing by coupling on the PBS with zero phase difference of interference. The detection system involves a pair of detectors with the photo electric diode, a half wave plate, a quarter wave plate, a PBS and a power combiner/substractor. The variances of the three Stokes operators ($\hat{S}_0$, $\hat{S}_1$, and $\hat{S}_2$) with squeezing of 4.0 dB, and anti-squeezing of 9.0 dB at the analysis frequency of 3.0 MHz have been experimentally measured.

2.2. Preparation of CV Polarization Entangled States of Optical Modes

The concepts of CV polarization squeezing have been extended to CV polarization entanglement.[38] The CV polarization entanglement can be efficiently generated and manipulated, meanwhile its measurement is independent on the local oscillator.[35] The polarization entanglement between two optical modes matching the optical fiber transmission window has been realized with the asymmetric fiber-optic Sagnac interferometer. Besides the application of polarization in quantum channel, squeezed state resonant with atom absorption line is demanding for quantum node. The polarization entangled state has been generated in high finesse optical cavity enhanced cold cesium atoms.[43] The sub-threshold OPAs and beam splitter network can produce bipartite polarization entangled optical modes. And the bipartite CV polarization entanglement resonant with rubidium atom absorption line has been obtained by transforming the quadrature entangled state into polarization entanglement on beam splitter network.[42]

Figure 2 shows the schematic of generating bipartite CV polarization entangled optical modes.[45] As mentioned above, the external cavity enhanced SHG outputs 398 nm lasers. The two identical sub-threshold OPAs pumped by 398 nm laser produce a pair of spatially separated quadrature amplitude squeezed states of optical modes, which are coupled on a 1:1 beam splitter to form a EPR entangled state. This pair of entangled optical modes is coupled with two strong coherent states of optical modes. With the extended inseparability criterion of CV bipartite polarization entanglement,[44,79,80] the CV polarization entangled state is experimentally verified. The normalized sum of correlation variances is less than 1 at the analyzing frequency between 1.8 and 6.5 MHz; and the normalized sum of correlation variances can be 0.5 at the analyzing frequency of 3 MHz.

The multipartite polarization entangled optical modes can directly interact with the spin states of multiple atomic ensembles, which can be conveniently used to transfer and store quantum states across atomic ensemble based quantum network. The multipartite polarization entanglement of optical modes resonant with D1 line of rubidium atoms has been generated by transforming the three CV quadrature entangled optical modes to polarization entanglement on a beam splitter network.[45] The

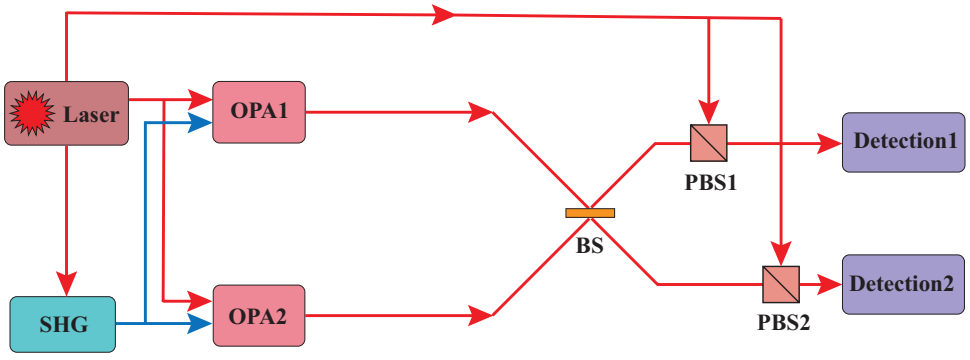

Figure 2. Schematic of generating bipartite CV polarization entangled optical modes. Laser system, a titanium sapphire laser pumped by green laser; SHG system, an external cavity enhanced second harmonic generator; OPAs, optical parametric amplifiers; BS, beam splitters; PBS, polarization beam splitters; detection system, measurement of Stokes operators of optical modes.

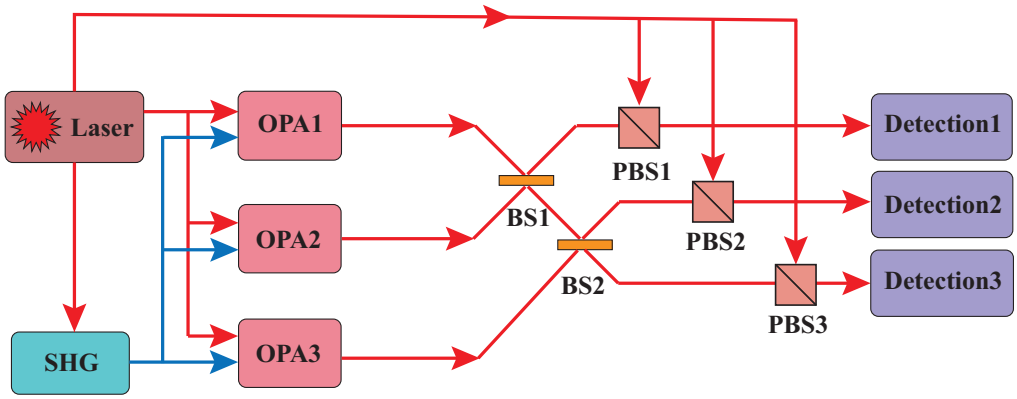

Figure 3. Schematic of generating tripartite CV polarization entangled optical modes. Laser system, a titanium sapphire laser pumped by green laser; SHG system, an external cavity enhanced second harmonic generator; OPAs, optical parametric amplifiers; BS, beam splitters; PBS, polarization beam splitters; detection system, measurement of Stokes operators of optical modes.

output state satisfies the inseparability criteria[47] and the genuine multipartite entangled criteria proposed by Teh and Reid.[46] The multipartite inseparability criteria for quadrature entanglement have been extended to the multipartite inseparability criteria for polarization entanglement, as

$$I_1 = \frac{\Delta^2(\hat{S}_{2d2} - \hat{S}_{2d3}) + \Delta^2(g_1\hat{S}_{3d1} + \hat{S}_{3d2} + \hat{S}_{3d3})}{4|\alpha_c^2 - \alpha_\alpha^2|} \geq 1, \quad (3)$$

$$I_2 = \frac{\Delta^2(\hat{S}_{2d1} - \hat{S}_{2d3}) + \Delta^2(\hat{S}_{3d1} + g_2\hat{S}_{3d2} + \hat{S}_{3d3})}{4|\alpha_c^2 - \alpha_\alpha^2|} \geq 1,$$

$$I_3 = \frac{\Delta^2(\hat{S}_{2d1} - \hat{S}_{2d2}) + \Delta^2(\hat{S}_{3d1} + \hat{S}_{3d2} + g_3\hat{S}_{3d3})}{4|\alpha_c^2 - \alpha_\alpha^2|} \geq 1$$

where I_i (i = 1,2,3) is the sum of normalized correlation variances, and g_i (i = 1,2,3) is the optimal gain factor. When any two of the above inequalities are unsatisfied, the three optical modes will be in CV polarization GHZ-like entangled state. For the genuine tripartite polarization entanglement, the inequality $I_1+I_2+I_3 \geq 2$ must be violated.

Figure 3 demonstrates the schematic of generating tripartite CV polarization entangled optical modes.[48] Three identical subthreshold OPAs pumped by 398 nm laser output three optical modes with quadrature amplitude squeezed states, which are coupled on a beam splitter network to form a GHZ-like quadrature entangled state. These quadrature entangled optical modes are transformed into CV polarization entangled optical modes by coupling with three strong coherent states of lasers on three PBSs. The correlation variances are all below the corresponding QNL at the frequency between 1.3 and 6.0 MHz. At the optimal analyzing frequency, $I_1 = 0.42\pm0.08$, $I_2 = 0.41\pm 0.08$, $I_3 = 0.42\pm0.08$, and $I_1+I_2+I_3 = 1.25\pm0.07$, which means both the criteria for tripartite inseparability and genuine tripartite entanglement are violated. This scheme can be extended to entangle CV polarization of more modes.

The three color quadrature entangled optical modes have been obtained by means of cascaded optical parametric oscillators operating above threshold. By coupling the resulting three color quadrature entangled optical modes with three strong coherent states on beam splitter network, the three color polarization entangled state can be generated.[47]

3. Generation and Storage of Entanglement of Spatially Separated Atomic Ensembles

The flying photons or optical modes are the best quantum information carrier, and optical fiber or orbiting satellites are the natural quantum channels. The stationary atomic ensembles are used as processor and memory of quantum information at quantum nodes.[81] Especially, atomic ensembles have the advantage of the collective enhancement of light and atom interaction as well as good quantum coherent, which enable to store and process quantum information.[82–86] It is crucial for the practical applications of quantum network to entangle the multiple spatially separated quantum memories, and at a user-controlled moment to transfer the stored entanglement to released signal optical modes which can be used for the conveyance of quantum information through quantum channels.

To entangle more quantum nodes is necessary for quantum networks. Quantum memory for entangled sidebands of optical mode enables to entangle two quantum nodes.[48] The generation and storage of deterministic quantum entanglement among three spatially separated atomic ensembles have been experimentally demonstrated, which can also be transferred into released signal optical modes for entanglement verification and further applications. The off-line prepared tripartite entangled optical modes are stored in three distant atomic ensembles, which entangle the atomic spin waves via EIT interaction. Then the entanglement stored in three atomic ensembles can be transferred into a three spatially separated released signal optical modes. The verification of entanglement among three released signal optical modes demonstrates that the quadrature amplitudes and phases of three atomic ensembles are in an entangled state and these atomic ensembles have the capacity to preserve multipartite entanglement. The presented scheme has good storage and retrieval scalability of non-classical light and can be directly extended to quantum networks with more nodes.

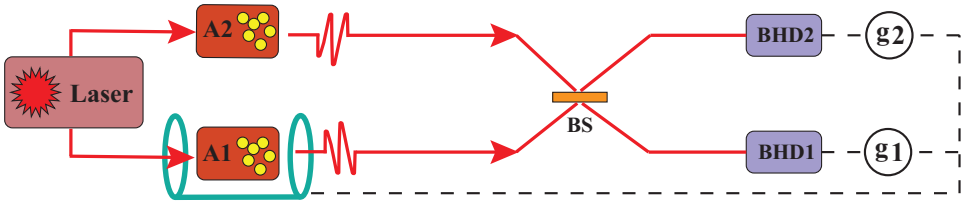

Figure 4. Schematic of entangling two atomic ensembles by means of hybrid entanglement swapping. Laser system, a titanium sapphire laser pumped by green laser; Ai, atomic ensembles, BS, beam splitters; BHD, balanced homodyne detection system, measurement of Stokes operators of optical modes.

3.1. EIT Quantum Memory for Non-Classical Optical Mode

When quantum fields propagate in EIT media, which forms the dark-state polarizations, and in this process the quantum state of light can be ideally transferred to atomic spin waves and vice versa. According to the dark state polariton theory, EIT memory is a well-known memory approach, which can on demand transfer quantum state between light and atomic ensembles. When control optical modes are adiabatically switched off, the transferring relations of quadrature amplitude and phase from input optical modes to atomic spin waves. Thus the EIT effects can be used to generate and store the nonclassical states in atomic ensembles.

Initially, quantum memory for coherent state has been demonstrated in rubidium atomic vapor cell.[87] The non-classical state of light is essential resource of implementing quantum information technology, which can improve the processing capacity of quantum information, increase the communication security, the sensitivity and resolution of precision measurement. Quantum memory for non-classical state of light is required for the development of quantum network. EIT technique can be applied in preserving the non-classical state of light because of the low excess memory noise; otherwise, quantum state will be merged in the excess memory noise. Especially, quantum memories for quantum states of light are demanding for implementing quantum network, and quantum storages of squeezed and entangled states have been widely investigated.[61,62]

The Hamiltonian of EIT memory is beam splitter type, and expressed as $H_{\mathrm{EIT}} = i\hbar\kappa A_C \hat{a}\hat{S}^{+} - i\hbar\kappa A_C \hat{a}^{+}\hat{S}$. When both the input signal and control optical modes are turned on, the group velocity of input signal optical mode is significantly reduced due to EIT effect and the input signal optical mode is compressed into the atomic ensemble. At the moment that the whole input signal optical mode is completely entered the atomic ensemble, the control optical mode is turned off and quantum state of signal optical mode is transferred into that of atomic spin wave, which are expressed as

$$\hat{X}_{Aj} = \sqrt{\eta_{\mathrm{M}}}\hat{X}_{Lj} + \sqrt{1-\eta_{\mathrm{M}}}\hat{X}_{Aj}^{\mathrm{vac}}, \tag{4}$$

$$\hat{P}_{Aj} = \sqrt{\eta_{\mathrm{M}}}\hat{P}_{Lj} + \sqrt{1-\eta_{\mathrm{M}}}\hat{P}_{Aj}^{\mathrm{vac}}$$

where η_{M} is the writing efficiency in quantum memory, and the unavoidable noise is introduced to atomic spin waves due to the limited writing efficiency. During the lifetime, the quantum state of input signal optical mode can be preserved in atomic ensemble. At the user controlled time, the control optical mode is switched on again, so that the signal mode is released from atomic ensemble and the quantum state of atomic spin wave is transferred into that of the released signal optical mode, whose expressions of reading process are

$$\hat{X}_{Lj} = \sqrt{\eta'_{\mathrm{M}}}\hat{X}_{Aj} + \sqrt{1-\eta'_{\mathrm{M}}}\hat{X}_{Lj}^{\mathrm{vac}}, \tag{5}$$

$$\hat{P}_{Lj} = \sqrt{\eta'_{\mathrm{M}}}\hat{P}_{Aj} + \sqrt{1-\eta'_{\mathrm{M}}}\hat{P}_{Lj}^{\mathrm{vac}}$$

where η'_{M} is the reading efficiency in quantum memory. The quantum performance of quantum memory can be verified by checking the quantum character of released signal optical mode.

3.2. Entanglement Between Two Atomic Ensemble Memories

The entanglement between two macroscopic objects has been implemented based on the QND measurement[55] and dispassion mechanism.[73] Quantum state transferring from CV entangled optical modes to atomic spin waves is a distinctive approach to entangle multiple quantum nodes which has been proved in a deterministic version. Quantum state transferring of CV entanglement from two sidebands of optical modes to two atomic ensembles enables to entangle these two atomic ensembles.[36]

Two macroscopic atomic ensembles can be entangled by means of hybrid entanglement swapping. The schematic of entangling two atomic ensembles in such approach is shown in **Figure 4**.[88] Atom and light hybrid entanglement swapping can deterministically entangle two spatially separated atomic ensembles, which involve two atomic ensembles with radio frequency coils, an 1:1 optical beam splitter, and two BHDs. Two sets of entanglements between atomic ensembles and optical modes are generated by means of the spontaneous Raman scattering. These two Stokes optical modes generated by the spontaneous Raman scattering are interfered at the 1:1 optical beam splitter with 0 phase difference, and the interfered optical modes from the output port of beam splitter are measured by two BHDs. The quadrature amplitude can be measured if the relative phase is locked at 0; the quadrature phase can be measured while the relative phase is locked at π /2. When the measured quadrature amplitude and phase are fed forward to two radio frequency coils of atomic ensembles via two classical channels, these two spatially separated atomic ensembles are unconditionally entangled. By applying the reading process, the anti-Stokes optical modes are released from the atomic ensembles, which can be used to verify the entanglement between these two atomic ensembles. According to the inseparability criteria,[79,80] these two atomic ensembles

are entangled, if the sum of correlation variances of the released signal optical modes is less than QNL.[9] By optimizing the gain factor of feed forward, the optimal entanglement between these two atomic ensembles can be obtained.

3.3. Establishment and Storage of Entanglement Among Multiple Atomic Ensembles

To entangle multiple atomic ensembles is a long standing goal of quantum network, which enables to realize the distributed quantum computation, and distributed quantum sensing. Measurement induced entanglement among four atomic memories has been realized to form a W state, and is verified by means of entanglement transfer from atomic spin waves to released optical modes.

Three modes of an optical GHZ-like entangled state are off-line prepared by means of three OPAs and beam splitter network. Quantum entanglement among three spatially separated quantum nodes is experimentally generated and stored by transferring off-line prepared entanglement of optical modes into atomic ensembles. Within storage lifetime, the tripartite GHZ-like entanglement can be preserved in three atomic ensembles, and then controllably converted into three released signal optical modes which can be transmitted through quantum channels. The tripartite GHZ-like entangled optical modes by coupling three squeezed vacuum states are created by three OPAs on two beam splitters and distributed to three atomic ensembles with spatial distance of 2.6 m. By means of EIT memory, GHZ-like entangled state is transferred from optical modes to atomic ensembles. At user controlled time, which should be during the memory lifetime, quantum state can be transferred from atomic ensembles to released signal optical modes again in the quantum reading process. The released signal optical modes can be used to verify the quantum performance among these three atomic ensembles. Finally, entanglement among released optical modes is measured by three sets of BHDs. According to the inseparability criteria for multipartite entanglement, these three atomic ensembles are entangled, if any two of the sums of correlation variances of the released signal optical modes are less than QNL. The full tripartite inseparability criteria for released signal optical modes are derived from.[89] If the tripartite entangled optical modes are stored in three atomic ensembles, these atomic ensembles will be entangled, as follows

$$I_{A1} = \frac{\Delta^2(\hat{S}_{A2} - \hat{S}_{A3}) + \Delta^2(g_{A1}\hat{S}_{A1} + \hat{S}_{A2} + \hat{S}_{A3})}{2} \geq 1, \quad (6)$$

$$I_{A2} = \frac{\Delta^2(\hat{S}_{A1} - \hat{S}_{A3}) + \Delta^2(\hat{S}_{A1} + g_{A2}\hat{S}_{A2} + \hat{S}_{A3})}{2} \geq 1,$$

$$I_{A3} = \frac{\Delta^2(\hat{S}_{A1} - \hat{S}_{A2}) + \Delta^2(\hat{S}_{A1} + \hat{S}_{A2} + g_{A3}\hat{S}_{A3})}{2} \geq 1$$

where g_{Ai} (i = 1, 2, 3) is the optimal gain factor for quantum entanglement among three atomic ensembles. When any two inequalities are not satisfied, the three atomic ensembles are in GHZ-like entangled state. In reading process of quantum memory, quantum states of atomic spin waves are transferred into those of released signal optical modes. The quantum entanglement among three atomic ensembles is verified by checking the quantum entanglement among three released signal optical modes, as follows

$$I_{L1} = \frac{\Delta^2(\hat{S}_{L2} - \hat{S}_{L3}) + \Delta^2(g_{L1}\hat{S}_{L1} + \hat{S}_{L2} + \hat{S}_{L3})}{2} \geq 1, \quad (7)$$

$$I_{L2} = \frac{\Delta^2(\hat{S}_{L1} - \hat{S}_{L3}) + \Delta^2(\hat{S}_{L1} + g_{L2}\hat{S}_{L2} + \hat{S}_{L3})}{2} \geq 1,$$

$$I_{L3} = \frac{\Delta^2(\hat{S}_{L1} - \hat{S}_{L2}) + \Delta^2(\hat{S}_{L1} + \hat{S}_{L2} + g_{L3}\hat{S}_{L3})}{2} \geq 1$$

where g_{Li} (i = 1, 2, 3)is the optimal gain factor for quantum entanglement among three released signal optical modes. When any two inequalities are not satisfied, the three released signal optical modes are in entangled state which furthermore demonstrate there is quantum entanglement among three atomic ensembles.

Figure 5 describes the experimental schematics for generation and storage of entanglement among three spatially separated atomic ensembles.[74] A Ti:Sapphire laser pumped by a single frequency solid state laser outputs 795 nm laser with 3 Watts, which is used as the fundamental wave laser of the SHG, input seeded optical mode of three OPAs, and local oscillation modes of BHD, respectively. Three OPAs and external cavity enhanced SHG have the same bow tie ring configuration of two flat mirrors, two concave mirrors and a 1 mm × 2 mm × 10 mm PPKTP nonlinear crystal. The SHG outputs 398 nm laser to pump the three OPAs, which produce three squeezed vacuum modes. OPA1 operates at the parametric amplification to generate quadrature phase squeezed state, while both OPA2 and OPA3 run at the parametric de-amplification to produce quadrature amplitude squeezed state. The quadrature phase squeezed vacuum state from OPA1 and quadrature amplitude squeezed vacuum state from OPA2 are coupled at a 1:2 optical beam splitter with relative phase difference of 0, and then the output optical mode from this beam splitter and the quadrature amplitude squeezed vacuum state from OPA3 are coupled at a 1:1 optical beam splitter with relative phase difference of 0. Three narrow band entangled optical beams tuned to the transition of rubidium D1 absorption line are obtained by linearly coupling three squeezed optical modes generated by three OPAs. The input signal modes for quantum memories are obtained by chopping the output optical modes from the optical beam splitter network using three pairs of AOMs. The control optical mode is generated by shifting the laser frequency of 6.8 GHz with a high speed EOM and amplified by a laser amplifier. The released signal optical modes from quantum memories are measured and analyzed based on three sets of BHDs. Three rubidium 87 atomic vapor cells with the anti-reflection coating at 795 nm and magnetic field shielding are used as the EIT memory media. The control optical modes with vertical polarization and input signal optical modes with horizontal polarization are coupled at Glan–Thompson polarizers, which are injected into three atomic ensembles. After the atomic ensembles, the control optical modes are filtered by the Glan–Thompson polarizers and a series of etalons. All the three released signal optical modes pass the Glan-Thompson polarizers and a series of etalons, which are measured by three sets of BHDs, respectively. Quantum memory is completed by controlling the time sequence, and at

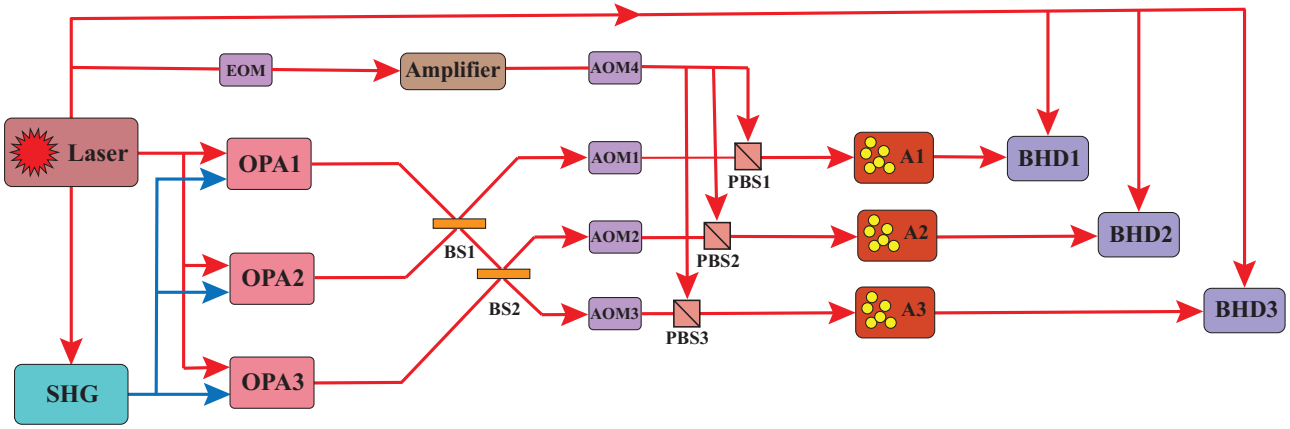

Figure 5. Schematic of generating and storing the tripartite entangled atomic ensembles. Laser system, a titanium sapphire laser pumped by green laser; SHG system, an external cavity enhanced second harmonic generator; OPAs, optical parametric amplifiers; Amplifier system, laser power amplifier; A, atomic ensembles; BS, beam splitters; PBS, polarization beam splitters; EOM, electro-optic modulator; AOM, acousto-optic modulator; BHD, balanced homodyne detection.

storage time of 1 μs the released signal optical modes are obtained by switching on the control optical modes again. All the OPAs and BHDs are interrupted locked by turning on the signal optical modes for most of time cycle. When the signal optical modes are turned off, quantum memory happens. When the input signal optical pulses of 500 ns are injected into atomic ensembles, the control optical modes are switched off so that the signal optical modes are stored in the atomic ensembles. After the storage time of 1 μs, the control modes are switched on again so that the signal optical modes are released from the atomic ensembles.

The excess noises in released signal modes are caused by the fluorescence, coherent emission, and spurious fluctuations in signal channels induced by the control optical modes.[62] Both EIT and four-wave mixing (FWM) effects are simultaneously generated in an ensemble with a certain detuning, and the control optical modes with a far detuned mode results in the undesired FWM noise. Thus, the EIT memory has to be operated with the proper detuning values of probe and control optical modes, the power of control optical beam and the temperature of atomic vapor, to avoid the excess noises, which will destroy quantum correlations among atomic ensembles. The correlation variances of input and released signal modes are measured with the help of three sets of BHDs. The normalized correlation variances sum for different combinations of quadrature components are $I_{L1} = I_{L2} = I_{L3} = 0.96 \pm 0.01$, when the gain factors are taken the optimal gains to minimize the corresponding correlation variances sum. Because the mapping efficiency is limited, the correlation variances of released optical modes are higher than that of input signal modes. The sum of correlation variances for three released signal modes is less than 1,[65] thus the entanglement among released signal modes is verified according to criterion inequalities and violates the criterion inequalities, which experimentally proves the existence of tripartite GHZ-like entanglement among three atomic ensembles.

The quality of GHZ-like entangled state among three atomic ensembles is mainly limited by the transferring efficiency and initial squeezed degree of squeezed vacuum. The better atom entanglement quality can be obtained, if higher memory efficiency and higher squeezed degree are employed. Transferring efficiency can be significantly improved by making use of the optical cavity enhancement technology without introducing excess noise.[90,91] The storage lifetime can be obviously increased by placing thermal atomic ensembles in paraffin coated cell. This scheme provides a new avenue to construct quantum internet and implement distributed quantum computation. The deterministic entanglement among three atomic ensembles based on EIT quantum memory with low excess memory noise has been established and stored, and our scheme is scalable which enables to entangle more atomic ensembles by employing more parties entangled optical modes. This work provides an avenue toward the practical applications of quantum network.

4. Conclusions and Outlook

In summary, we have reviewed the developments in the past few years on quantum network involving the atomic ensembles and non-classical light. The non-classical state of light is the building block of quantum information technology. The CV polarization non-classical state of optical modes, such as a squeezed state, an EPR entangled state, and a tripartite GHZ-like state, can interact directly with atomic spin and have been generated by means of OPAs and beam splitter networks. The unconditional generations of CV polarization non-classical states have been proven. Due to its advantages in interaction between atomic ensemble and non-classical light, the resulting CV polarization non-classical state can play more prominent roles in practical applications of quantum network. For instance, CV polarization non-classical states can be stored in atomic ensembles with the advantage of direct interaction between Stokes operators of atom and light. The CV polarization entangled states can be used to teleport quantum information over a long distance, and realize the distributed quantum sensing across quantum network, because the local oscillation free measurement is suitable for long distance tasks.

On the other hand, quantum memory with both high efficiency and low excess noise is necessary for establishing and storing multipartite entangled state in quantum nodes. There are still many technologies to improve the performance of quantum

memory. By means of the optical cavity enhancement technology, the atomic spin wave to released optical photons conversion efficiency can be improved and the excess noise in quantum memory can be reduced.[90,91] The magnetic noise mainly limits the memory lifetime, and can be improved by optimizing the structure of magnetic shielding. Also the cell-wall paraffin coating can extend the memory lifetime of warm atom in the cell, and the millisecond-scale lifetime in the paraffin coated atomic vapor cell can be realized.[36,51] Quantum entanglement of remote quantum nodes over long distances can advance the applications of quantum network. At present the maximal distance between two quantum nodes is in city scale over dozens of kilometers. The atom and photon entanglement is efficiently produced in optical cavity and then quantum frequency conversion is used to shift the atomic wavelength to telecommunication wavelength for long distance distribution. The entanglement over 50 km is obtained via single-photon interference.[92]

High performance quantum memory holds promise for the high fidelity quantum information processing and high precision quantum metrology. By integrating smaller quantum modules to a larger computing cluster, distributed quantum structure can be used to solve the unavoidable decoherence problem in a large-scale quantum processor, where the quantum memory based element registers can preserve, control and read out quantum states.[93] Besides, the ultimate measurement sensitivity is restricted by the QNL. Spin squeezing generated by storing the squeezed optical mode provides an effective approach to overcome this limit, and enables to improve the sensitivity of atomic magnetometry.[51] There are still interesting topics to investigate how these high quality quantum resources can promote practical applications of quantum network.

Acknowledgements

This research was supported by the Key Project of the National Key R&D program of China (Grant No. 2016YFA0301402), the National Natural Science Foundation of China (Grants No. 61775127, No. 61925503, No. 11904218, No. 11654002, and No. 11834010), the Program for the Innovative Talents of Higher Education Institutions of Shanxi, the Program for the Outstanding Innovative Teams of Higher Learning Institutions of Shanxi, Natural Science Foundation of Shanxi Province, China (201801D221009), the Program for Sanjin Scholars of Shanxi Province, and the fund for Shanxi "1331 Project" Key Subjects Construction.

Conflict of Interest

The authors declare no conflict of interest.

Keywords

multipartite polarization entanglement, quantum entanglement, quantum memory, quantum nodes

Received: May 26, 2021
Revised: July 1, 2021
Published online:

[1] J. Yin, Yuan Cao, Y.-H. Li, S.-K. Liao, L. Zhang, J.-G. Ren, W.-Q. Cai, W.-Y. Liu, B. Li, H. Dai, G.-B. Li, Q.-M. Lu, Y.-H. Gong, Y. Xu, S.-L. Li, F.-Z. Li, Y.-Y. Yin, Z.-Q. Jiang, M. Li, J.-J. Jia, G. Ren, D. He, Y.-L. Zhou, X.-X. Zhang, N. Wang, X. Chang, Z.-C. Zhu, N.-L. Liu, Y.-A. Chen, C.-Y. Lu, et al., *Science* **2017**, *356*, 1140.
[2] M.-R. Huo, J.-L. Qin, J.-L. Cheng, Z.-H. Yan, Z.-Z. Qin, X.-L. Su, X.-J. Jia, C.-D. Xie, K.-C. Peng, *Sci. Adv.* **2018**, *4*, eaas9401.
[3] M. Hosseini, B. M. Sparkes, G. Campbell, P. K. Lam, B. C. Buchler, *Nat. Commun.* **2011**, *2*, 174.
[4] V. Parigi, V. Ambrosio, C. Arnold, L. Marrucci, F. Sciarrino, J. Laurat, *Nat. Commun.* **2015**, *6*, 7706.
[5] Z.-H. Yan, X.-J. Jia, *Quantum Sci. Technol.* **2017**, *2*, 024003.
[6] Y.-F. Pu, N. Jiang, W. Chang, H.-X. Yang, C. Li, L. M. Duan, *Nat. Commun.* **2017**, *8*, 15359.
[7] G. Colangelo, F. M. Ciurana, L. C. Bianchet, R. J. Sewell, M. W. Mitchell, *Nature* **2017**, *543*, 525.
[8] H. P. Specht, C. Nolleke, A. Reiserer, M. Uphoff, E. Figueroa, S. Ritter, G. Rempe, *Nature* **2011**, *473*, 190.
[9] A. Facon, E. K. Dietsche, D. Grosso, S. Haroche, J. M. Raimond, M. Brune, S. Gleyzes, *Nature* **2016**, *535*, 262.
[10] A. Stute, B. Casabone, P. Schindler, T. Monz, P. O. Schmidt, B. Brandstater, T. E. Northup, R. Blatt, *Nature* **2012**, *485*, 482.
[11] D. Hucul, I. V. Inlek, G. Vittorini, C. Crocker, S. Debnath, S. M. Clark, C. Monroe, *Nat. Phys.* **2014**, *11*, 37.
[12] V. Fiore, Y. Yang, M. C. Kuzyk, R. Barbour, L. Tian, H. Wang, *Phys. Rev. Lett.* **2011**, *107*, 133601.
[13] H. Lee, M. G. Suh, T. Chen, Li J, S. A. Diddams, K. J. Vahala, *Nat. Commun.* **2013**, *4*, 2468.
[14] R. Riedinger, S. Hong, R. A. Norte, J. A. Slater, J. Shang, A. G. Krause, V. Anant, M. Aspelmeyer, S. Grolacher, *Nature* **2016**, *530*, 313.
[15] S. Kiesewetter, R. Y. Teh, P. D. Drummond, M. D. Reid, *Phys. Rev. Lett.* **2017**, *119*, 023601.
[16] E. Flurin, N. Roch, J. D. Pillet, F. Mallet, B. Huard, *Phys. Rev. Lett.* **2015**, *114*, 090503.
[17] E. Saglamyurek, N. Sinclair, J. Jin, J. A. Slater, D. Oblak, F. Bussieres, M. George, R. Ricken, W. Sohler, W. Tittel, *Nature* **2011**, *469*, 512.
[18] M. Zhong, M. P. Hedges, R. L. Ahlefeldt, J. G. Bartholomew, S. E. Beavan, S. E. Wittig, J. J. Longdell, M. J. Sellars, *Nature* **2015**, *517*, 177.
[19] Z.-B. Chen, C.-Y. Lu, H. Weinfurter, A. Zeilinger, M. Żukowsk, *Rev. Mod. Phys.* **2012**, *84*, 777.
[20] S. L. Braunstein, P. van Loock, *Rev. Mod. Phys.* **2005**, *77*, 513.
[21] Z. H. Yan, J. L. Qin, Z. Z. Qin, X. L. Su, X. J. Jia, C. D. Xie, K. C. Peng, *Fundamental Res.* **2021**, *1*, 43.
[22] D. Bouwmeester, J.-W. Pan, K. Mattle, M. Eibl, H. Weinfurter, A. Zeilinger, *Nature* **1997**, *390*, 575.
[23] A. Furusawa, J. L. Soensen, S. L. Braunstein, C. A. Fuchs, H. J. Kimble, E. S. Polzik, *Science* **1998**, *282*, 706.
[24] J.-W. Pan, D, Bouwmeester, H. Weinfurter, A. Zeilinger, *Phys. Rev. Lett.* **1998**, *80*, 3891.
[25] X.-J. Jia, X.-L. Su, Q. Pan, J.-R. Gao, C.-D. Xie, K.-C. Peng, *Phys. Rev. Lett.* **2004**, *93*, 250503.
[26] S. Takeda, M. Fuwa, P. van Loock, A. Furusawa, *Phys. Rev. Lett.* **2015**, *114*, 100501.
[27] Y.-A. Chen, A.-N. Zhang, Z. Zhao, X. Q. Zhou, C.-Y. Lu, C. Z. Peng, T. Yang, J.-W. Pan, *Phys. Rev. Lett.* **2005**, *95*, 200502.
[28] A. M. Lance, T. Symul, W. P. Bowen, B. C. Sanders, P. K. Lam, *Phys. Rev. Lett.* **2004**, *92*, 177903.
[29] Y.-Y. Zhou, J. Yu, Z.-H. Yan, X.-J. Jia, J. Zhang, C.-D. Xie, K.-C. Peng, *Phys. Rev. Lett.* **2018**, *121*, 150502.
[30] X.-D. Cai, D. Wu, Z.-S. Su, M.-C. Chen, X.-L. Wang, L. Li, N.-L. Liu, C.-Y. Lu, J.-W. Pan, *Phys. Rev. Lett.* **2015**, *114*, 110504.
[31] X.-L. Su, S.-H. Hao, X.-W. Deng, L.-Y. Ma, M.-H. Wang, X.-J. Jia, C.-D. Xie, K.-C. Peng, *Nat. Commun.* **2013**, *4*, 2828.
[32] X.-J. Zuo, Z.-H. Yan, Y.-N. Feng, J.-X. Ma, X.-J. Jia, C.-D. Xie, K.-C. Peng, *Phys. Rev. Lett.* **2020**, *124*, 173602.

[33] L.-A. Wu, H. J. Kimble, J. H. Hall, H. F. Wu, *Phys. Rev. Lett.* **1986**, *57*, 2520.
[34] Z.-Y. Ou, S. F. Pereira, H. J. Kimble, K. C. Peng, *Phys. Rev. Lett.* **1992**, *68*, 3663.
[35] T. S. Iskhakov, I. N. Agafonov, M. V. Chekhova, G. Leuchs, *Phys. Rev. Lett.* **2012**, *109*, 150502.
[36] K. Jensen, W. Wasilewski, H. Krauter, T. Fernholz, B. M. Nielsen, M. Owari, M. B. Plenio, A. Serafini, M. M. Wolf, E. S. Polzik, *Nat. Phys.* **2011**, *7*, 13.
[37] C. Peuntinger, B. Heim, C. R. Muller, C. Gabriel, C. Marquardt, G. Leuchs, *Phys. Rev. Lett.* **2014**, *113*, 060502.
[38] N. Korolkova, G. Leuchs, R. Loudon, T. C. Ralph, C. Silberhorn, *Phys. Rev. A* **2002**, *65*, 052306.
[39] W. P. Bowen, R. Schnabel, H. A. Bachor, P. K. Lam, *Phys. Rev. Lett.* **2002**, *88*, 093601.
[40] T. Iskhakov, M. V. Chekhova, G. Leuchs, *Phys. Rev. Lett.* **2009**, *102*, 183602.
[41] V. Josse, A. Dantan, L. Vernac, A. Bramati, M. Pinard, E. Giacobino, *Phys. Rev. Lett.* **2003**, *91*, 103601.
[42] L. Wu, Y.-H. Liu, R.-J. Deng, Z.-H. Yan, X.-J. Jia, K.-C. Peng, *J. Opt. Soc. Am. B* **2016**, *33*, 2296.
[43] V. Josse, A. Dantan, A. Bramati, M. Pinard, E. Giacobino, *Phys. Rev. Lett.* **2004**, *92*, 123601.
[44] W. P. Bowen, N. Treps, R. Schnabel, P. K. Lam, *Phys. Rev. Lett.* **2002**, *89*, 253601.
[45] L. Wu, Y.-H. Liu, R.-J. Deng, Z.-H. Yan, X.-J. Jia, *Acta Opt. Sin.* **2017**, *37*, 0527001.
[46] R. Y. Teh, M. D. Reid, *Phys. Rev. A* **2014**, *90*, 062337.
[47] Z.-H. Yan, X,-J. Jia, *J. Opt. Soc. Am. B* **2015**, *32*, 2139.
[48] L. Wu, Z.-H. Yan, Y.-H. Liu, R.-J. Deng, X.-J. Jia, C.-D. Xie, K.-C. Peng, *Appl. Phys. Lett.* **2016**, *108*, 161102.
[49] L.-M. Duan, M. D. Lukin, J. I. Cirac, P. Zoller, *Nature* **2001**, *414*, 413.
[50] D. Awschalom, K. K. Berggren, H. Bernien, S. Bhave, L. D. Carr, P. Davids, S. E. Economou, D. Englund, A. Faraon, M. Fejer, S. Guha, M. V. Gustafsson, E. Hu, L. Jiang, J. Kim, B. Korzh, P. Kumar, P. G. Kwiat, M. Loncar, M. D. Lukin, D. A. B. Miller, C. Monroe, S. W. Nam, P. Narang, J. S. Orcutt, M. G. Raymer, A. H. Safavi-Naeini, M. Spiropulu, K. Srinivasan, S. Sun, J. Vuckovi, E. Waks, R. Walsworth, A. M. Weiner, Z. Zhang, *PRX Quantum* **2021**, *2*, 017002.
[51] H. Bao, J. Duan, S. Jin, X. Lu, P. Li, W. Qu, M. Wang, I. Novikova, E. E. Mikhailov, K.-F. Zhao, K. Mølmer, H. Shen, Y. Xiao, *Nature* **2020**, *581*, 159.
[52] M. Fleischhauer, A. Imamoglu, J. P. Marangos, *Rev. Mod. Phys.* **2005**, *77*, 633.
[53] D. F. Phillips, A. Fleischhauer, A. Mair, R. L. Walsworth, *Phys. Rev. Lett.* **2001**, *86*, 783.
[54] M. Fleischhayer, M. Lukin, *Phys. Rev. A* **2002**, *65*, 022314.
[55] B. Julsgaard, J. Sherson, J. I. Cirac, J. Fiurasek, E. S. Polzik, *Nature* **2004**, *432*, 482.
[56] G. Hetet, J. J. Longdell, M. J. Sellars, P. K. Lam, B. C. Buchler, *Phys. Rev. Lett.* **2008**, *101*, 203601.
[57] S. Moiseev, S. Kroll, *Phys. Rev. Lett.* **2001**, *87*, 173601.
[58] L.-M. Duan, M. D. Lukin, J. I. Cirac, P. Zoller, *Nature* **2001**, *414*, 413.
[59] Z.-S. Yuan, Y.-A. Chen, B. Zhao, S. Chen, J. Schmiedmayer, J.-W. Pan, *Nature* **2008**, *454*, 1098.
[60] H. de Riedmatten, M. Afzelius, Matthias U. Staudt, C. Simon, N. Gisin, *Nature* **2008**, *456*, 773.
[61] K. Honda, D. Akamatsu, M. Arikawa, Y. Yokoi, K. Akiba, S. Nagatsuka, T. Tanimura, A. Furusawa, M. Kozuma, *Phys. Rev. Lett.* **2008**, *100*, 093601.
[62] J. Appel, E. Figueroa, D. Korystov, M. Lobino, A. I. Lvovsky, *Phys. Rev. Lett.* **2008**, *100*, 093602.
[63] T. D. Ladd, F. Jelezko, R. Laflamme, Y. Nakamura, C. Monroe, J. L. O'Brien, *Nature* **2010**, *464*, 45.
[64] N. Sangouard, C. Simon, H. D. Riedmatten, N. Gisin, *Rev. Mod. Phys.* **2011**, *83*, 33.
[65] H. J. Kimble, *Nature* **2008**, *453*, 1023.
[66] C. W. Chou, H. de Riedmatten, D. Felinto, S. V. Polyakov, S. J. van Enk, H. J. Kimble, *Nature* **2005**, *438*, 828.
[67] D. N. Matsukevich, T. Chanelière, S. D. Jenkins, S.-Y. Lan, T. A. B. Kennedy, A. Kuzmich, *Phys. Rev. Lett.* **2006**, *96*, 030405.
[68] K. S. Choi, H. Deng, J. Laurat, H. J. Kimble, *Nature* **2008**, *452*, 67.
[69] W. Zhang, D.-S. Ding, M.-X. Dong, S. Shi, K. Wang, S.-L. Liu, Y. Li, Z.-Y. Zhou, B.-S. Shi, G.-C. Guo, *Nat. Commun.* **2016**, *7*, 13514.
[70] K. S. Choi, A. Goban, S. B. Papp, S. J. Van Enk, H. J. Kimble, *Nature* **2010**, *468*, 412.
[71] B. Jing, X.-J. Wang, Y. Yu, P.-F. Sun, Y. Jiang, S.-J. Yang, W.-H. Jiang, X.-Y. Luo, J. Zhang, X. Jiang, X.-H. Bao, J.-W. Pan, *Nat. Photonics* **2019**, *13*, 210.
[72] B. Julsgaard, A. E. Kozhekin, E. S. Polzik, *Nature* **2001**, *413*, 400.
[73] H. Krauter, C. A. Muschik, K. Jensen, W. Wasilewski, J. M. Petersen, J. I. Cirac, E. S. Polzik, *Phys. Rev. Lett.* **2011**, *107*, 080503.
[74] Z.-H. Yan, L. Wu, X. Jia, Y. Liu, R. Deng, S. Li, H. Wang, C. Xie, K. Peng, *Nat. Commun.* **2017**, *8*, 718.
[75] P. Grangien, R. E. Slusheg, B. Yurke, A. LaPorta, *Phys. Rev. Lett.* **1987**, *59*, 2153.
[76] E. S. Polzik, J. Carri, H. J. Kimble, *Phys. Rev. Lett.* **1992**, *68*, 3020.
[77] M. Tse, H. Yu, N. Kijbunchoo, A. Fernandez-Galiana, P. Dupej, L. Barsotti, C. D. Blair, D. D. Brown, S. E. Dwyer, A. Effler, M. Evans, P. Fritschel, V. V. Frolov, A. C. Green, G. L. Mansell, F. Matichard, N. Mavalvala, D. E. McClelland, L. McCuller, T. McRae, J. Miller, A. Mullavey, E. Oelker, I. Y. Phinney, D. Sigg, B. J. J. Slagmolen, T. Vo, R. L. Ward, C. Whittle, R. Abbott, et al., *Phys. Rev. Lett.* **2019**, *123*, 231107.
[78] F. Acernese, M. Agathos, L. Aiello, A. Allocca, A. Amato, S. Ansoldi, S. Antier, M. Arène, N. Arnaud, S. Ascenzi, P. Astone, F. Aubin, S. Babak, P. Bacon, F. Badaracco, M. K. M. Bader, J. Baird, F. Baldaccini, G. Ballardin, G. Baltus, C. Barbieri, P. Barneo, F. Barone, M. Barsuglia, D. Barta, A. Basti, M. Bawaj, M. Bazzan, M. Bejger, et al., *Phys. Rev. Lett.* **2019**, *123*, 231108.
[79] L.-M. Duan, G. Giedke, J. I. Cirac, P. Zoller, *Phys. Rev. Lett.* **2000**, *84*, 2722.
[80] R. Simon, *Phys. Rev. Lett.* **2000**, *84*, 2726.
[81] K. Hammerer, A. S. Sorensen, E. S. Polzik, *Rev. Mod. Phys.* **2008**, *82*, 1041.
[82] J. Simon, H. Tanji, S. Ghosh, V. Vuletic, *Nat. Phys.* **2007**, *3*, 765.
[83] A. M. Marino, R. C. Pooser, V. Boyer, P. D. Lett, *Nature* **2009**, *457*, 859.
[84] Z.-X. Xu, Y. Wu, L. Tian, L. Chen, Z. Zhang, Z. Yan, S. Li, H. Wang, C. Xie, K. Peng, *Phys. Rev. Lett.* **2013**, *111*, 240503.
[85] Y.-H. Chen, M.-J. Lee, I.-C. Wang, S. Du, Y.-F. Chen, Y.-C. Chen, I. A. Yu, *Phys. Rev. Lett.* **2013**, *110*, 083601.
[86] V. Parigi, V. D'Ambrosio, C. Arnold, L. Marrucci, F. Sciarrino, J. Laurat, *Nat. Commun.* **2015**, *6*, 7706.
[87] M. Fleischhauer, M. D. Lukin, *Phys. Rev. Lett.* **2000**, *84*, 5094.
[88] Y.-H. Liu, Z.-H. Yan, X.-J. Jia, C.-D. Xie, *Sci. Rep.* **2016**, *6*, 25715.
[89] P. van Loock, A. Furusawa, *Phys. Rev. A* **2003**, *67*, 052315.
[90] S.-J. Yang, X.-J. Wang, X.-H. Bao, J.-W. Pan, *Nat. Photon.* **2016**, *10*, 381.
[91] D. J. Saunders, J. H. D. Munns, T. F. M. Champion, C. Qiu, K. T. Kaczmarek, E. Poem, P. M. Ledingham, I. A. Walmsley, J. Nunn, *Phys. Rev. Lett.* **2016**, *116*, 090501.
[92] Y. Yu, F. Ma, X.-Y. Luo, B. Jing, P.-F. Sun, R.-Z. Fang, C.-W. Yang, H. Liu, M.-Y. Zheng, X.-P. Xie, W.-J. Zhang, L.-X. You, Z. Wang, T.-Y. Chen, Q. Zhang, X.-H. Bao, J.-W. Pan, *Nature* **2020**, *578*, 240.
[93] S. Daiss, S. Langenfeld, S. Welte, E. Distante, P. Thomas, L. Hartung, O. Morin, G. Rempe, *Science* **2021**, *371*, 614.

Zhihui Yan received his B.S. degree (2006) and Ph.D. degree (2012) from Shanxi University, China. He has worked in Prof. Kunchi Peng's group at the Institute of Opto-electronics, Shanxi University since 2012. He has been working as a professor at Shanxi University since 2018. His research interests focus on the fields of the continuous-variable quantum optics and quantum information.